Journal of Colloid and Interface Science 436 (2014) 1–8

Contents lists available at ScienceDirect

Journal of Colloid and Interface Science

www.elsevier.com/locate/jcis

Retention of silica nanoparticles on calcium carbonate sands immersed in electrolyte solutions

Yan Vivian Li [a,*], Lawrence M. Cathles [b]

[a] Department of Design and Merchandising, Colorado State University, Fort Collins, CO 80523, United States
[b] Earth and Atmospheric Sciences, Cornell University, Ithaca, NY 14853, United States

ARTICLE INFO

Article history:
Received 10 June 2014
Accepted 31 August 2014
Available online 16 September 2014

Keywords:
Nanoparticle retention
Electrolyte solutions
Calcium carbonate (calcite)
Interfacial forces
Derjaguin–Landau–Verwey–Overbeek (DLVO) theory
Surface charge

ABSTRACT

Understanding nanoparticle–surface adhesion is necessary to develop inert tracers for subsurface applications. Here we show that nanoparticles with neutral surface charge may make the best subsurface tracers, and that it may be possible to used SiO_2 nanoparticle retention to measure the fraction of solid surface that has positive charge. We show that silica nanoparticles dispersed in NaCl electrolyte solutions are increasingly retained in calcium carbonate (calcite) sand-packed columns as the solution ionic strength increases, but are not retained if they are injected in pure water or Na_2SO_4 electrolyte solutions. The particles retained in the NaCl experiments are released when the column is flushed with pure water or Na_2SO_4 solution. AFM measurements on calcite immersed in NaCl solutions show the initial repulsion of a silica colloidal probe as the surface is approached is reduced as the solution ionic strength increases, and that at high ionic strengths it disappears entirely and only attraction remains. These AFM measurements and their interpretation with Derjaguin–Landau–Verwey–Overbeek (DLVO) theory shows the calcite surface charge is always negative for Na_2SO_4 solutions, but changes from negative to positive in a patchy fashion as the ionic strength of the NaCl solution increases. Since mixed-charge (patchy) surfaces may be common in the subsurface, nanoparticles with near-zero charge may make the best tracers.

1. Introduction

Aggregation and deposition of engineered nanomaterials is largely controlled by physicochemical interactions [1]. In drug delivery and in medical diagnosis it is critical that the nanoparticle remain in the blood long enough to reach target organs to be imaged or tumor cells to be treated [2]. The interactions of nanoparticles with biological units controls the formation of nanoparticle clusters on the membranes, and the formation of these clusters improves drug delivery efficiency [3]. The nanofabrication of electronic and optical devices depends on the interaction of nanostructured materials with fabricated devices. These interactions are affected by chemical conditions, and manipulation of these conditions allows the construction of the dyads, triads, strings, clusters, and other architectures that are the basis of a new generation of nano-devices and smart materials [4,5]. The size, shape, and composition of the particles and hydrodynamic conditions are important, but so also is the surface charge of the particles, and this is controlled by the chemistry of the surrounding solution (e.g. pH, ionic strength, and ionic composition) [1,3,5].

Size-dependence of nanoparticle adsorption has been reported for silica [6], gold [7], silver [8,11] and carbon nanotube particles [9]. The optimal size seems to be that which allows the ordered formation of nanoparticle monolayers [10]. The curvature of the surface of the nanoparticle could influence adsorption and the properties of the adsorbed particles [11]. Nanoparticles with different shapes interact differently with the same substrates. Pal et al. showed that antibacterial properties of silver nanoparticles undergo a shape-dependent interaction with bacteria [12].

Solution chemistry is a critical external factor controlling nanoparticle behavior [1,13]. The pH, ionic strength, and the ionic composition of the solution controls nanoparticle stability primarily by changing surface charge. Maintaining the solution within a range of pH and ionic strength is usually required to maintain a stable nanoparticle suspension. The width of the stability range depends on the nanoparticle chemistry and the ions in solution [14,15]. Increasing the ionic strength of a solution increases the nanoparticle retention in silica sand packed column [16,17], and the mix of aqueous ions affects particle retention [18,19]. Many nanoparticles such as silica, polystyrene latex, and TiO_2 have been injected into sand packed laboratory columns and into the subsurface, and it has been found that the mineralogy of the nanoparticle and the solid materials it contacts influence transport behavior

* Corresponding author. Fax: +1 970 491 4855.
E-mail address: yan.li@colostate.edu (Y.V. Li).

http://dx.doi.org/10.1016/j.jcis.2014.08.072
0021-9797/

[20]. Silica nanoparticles are not retained at all when passed through quartz sands and sandstone, but are slightly retained in limestone [1,21]. A slug of water can completely mobilize silica particles retained in a limestone packing [21]. Silica colloids and nanoparticles are the most commonly selected engineered nanomaterials for water treatment and contaminant remediation [22–24], and their behavior in porous rock media has been widely studied.

It has been possible to understand much of this behavior theoretically. The Derjaguin–Landau–Verwey–Overbeek (DLVO) theory predicts interfacial forces between a particle and a surface [16]. The interaction force is the sum of the van de Waals (VdW) and electrostatic double layer (EDL) interactions. The VdW forces are of relatively short-range and always present, but are not very sensitive to solution ionic strength. EDL forces are relatively long-range and are sensitive to solution ionic strength. To account for nanoparticle adsorption on organic surfaces, the DLVO theory has been extended to include repulsive steric force [25]. Hydrophilic and hydrophobic forces [26] and even magnetic force [27] can influence nanoparticle aqueous suspensions.

Nanoparticle–surface interaction in aqueous solutions has been investigated at nano scale using techniques such as X-ray diffraction [28], atomic force microscopy (AFM) [29], and quartz crystal microbalance (QCM) [30]. These methods directly measure the interactions of nanoparticles with solid surfaces and their molecular arrangement and ordering [31,32]. Nanoparticle–surface interactions in aqueous solutions have also been studied using columns packed with sands of various mineralogy. But few studies combine these methods, and we still lack a comprehensive and fundamental understanding of what controls particle retention in porous media.

In this paper, we study silica nanoparticle stickiness not only using column methods but also atomic force microscopy measurements and DLVO theory. First the retention of silica nanoparticles in both NaCl and Na_2SO_4 solutions is measured when silica particles dispersed in solution are passed through a calcite sand-packed column. We then make atomic force microscopy measurements between a silica colloidal AFM probe and calcite submerged in similar NaCl and Na_2SO_4 solution. The surface charge on the calcite surface is inferred from the AFM force profiles using the DLVO theory. The surface charge on the calcite is always negative for the Na_2SO_4 solutions and negative in low ionic strength NaCl solutions, but positive in higher ionic strength NaCl solutions. The NaCl column experiments suggest that this transition in surface charge occurs as the proportion of the calcite surface with positive charge increases as the NaCl ionic strength increases. Particles that electrostatically adhere to the areas with positive surface charge in high ionic strength NaCl solution can therefore be released when dilute solution are introduced and these areas of positive charge disappear. Our motivation in this and other studies is to develop non-interacting nanoparticle tracers for subsurface flow applications [33], and this paper follows up on a suggestion that near-zero particle charge (zeta potential) minimized particle retention [34]. The results of the experiments reported here indicates that zero charge nanoparticles may make the best non-reactive tracers because minerals with mixed surface charge will likely be common in the subsurface.

2. Materials and methods

2.1. Materials

2.1.1. SiO_2 nanoparticles

Green fluorescent SiO_2 nanoparticles were purchased from Corpuscular Inc. (Cold Spring, NY). The particle diameter was 87 ± 12 nm. The particle morphology and fluorescence spectrum are shown in Fig. S1 (Supporting Information).

2.1.2. Electrolyte solutions

The electrolyte solutions were prepared using analytical grade NaCl (Sigma–Aldrich) and Na_2SO_4 (anhydrous, granular, Mallinckrodt Chemicals) without further purification. The preparations are described in Text S1 (Supporting Information).

2.1.3. Calcite samples

The calcite (calcium carbonate) that was used in AFM measurements was iceland spar (calcite polymorph, Ward's Natural Science). A cold chisel was used to cleave off approximately a 1 cm cube of optically clear calcium carbonate crystal. This provides $\{10\bar{1}4\}$ cleavage surfaces that are atomically flat over several to tens of micrometers, a prerequisite for high-quality AFM measurements [35]. The $\{10\bar{1}4\}$ surfaces contain both Ca and CO_3 ions, making it charge neutral, and has a higher density of ions than other possible neutral planes, leading to its low surface energy and stable surfaces [36]. The sample preparation was done a day before the AFM measurements. The calcite sands that were used to pack the column were purchased from Specialty Mineral Inc., Lucerne Valley, CA. The sands contain 97% calcium carbonate. The average particles size is 300–500 μm.

2.2. Column design and experiments

The column experiments were conducted by passing tracer particle solutions through a transparent polycarbonate column filled with calcium carbonate sands (see Fig. S2, Supporting Information). The design of the column similar with previous column experiments [37] is described in Text S2 (Supporting Information).

A tracer solution is prepared which contains 100 ppm SiO_2 nanoparticles and either 0.5 mM, 10 mM, or 100 mM NaCl (or Na_2SO_4). The nanoparticle/electrolyte solution is pumped slowly into the bottom of the column using a peristaltic pump at a flow rate of 0.3 ml/min for a certain period of time so that a slug of tracer is introduced into the column. This tracer slug is followed by the same NaCl (or Na_2SO_4) solution without SiO_2 nanoparticles. After this, DI water is pumped through the column in some experiments as indicated. Effluent is collected every 4 min. The nanoparticle concentration of the effluent is determined using a previously-determined fluorescence – concentration calibration curve. Fluorescent spectroscopy (SpectroMax M5, Molecular Devices, LLC) is used to determine the relationship between SiO_2 particle concentration and particle fluorescence intensity (515 nm). The ratio of collected to injected particle concentrations is plotted against the pore volume throughput.

2.3. AFM measurements

An atomic force microscope system (NTEGRA Prima, NT-MDT, Zelenograd, Russian Federation) was employed to perform direct force measurements on the calcium carbonate submerged in liquid. Electrolyte (NaCl or Na_2SO_4) solution was added to a stainless steel cell where the calcium carbonate, which was glued to the bottom of the cell, was submerged. A SiO_2 colloidal AFM probe was purchased from Novascan Technologies. An amorphous SiO_2 colloid (5 μm in diameter) was attached on the end of the AFM cantilever, as shown in the SEM image in Fig. S3a (Supporting Information). The SiO_2 colloidal probe was used to directly measure the force between the silica colloid and the calcium carbonate surface as the colloid approached the surface. A 20 μm × 20 μm area of the submerged calcite surface was probed at 36 points by the AFM using the SiO_2 colloidal probe and the results averaged. The same 36 points were probed for all solutions. The geometry of the tip was examined with a scanning electron microscope before and after force measurements. This confirmed that the radius of the tip that contacts the calcite surface was roughly

80 nm in diameter, and same before and after the force measurements. The same tip was used for all measurements. According to the manufacturer the force constant of the cantilever was 0.35 N/m and this value was used by us under constant measurement conditions (e.g., constant tip approach velocity) without verification. Comparisons between solutions are thus valid, which is the important thing for this paper, but the absolute values of the force measurements are not necessarily correct.

Before the force measurements were made in each electrolyte solution, a 20 μm × 20 μm area of the submerged calcite surface was scanned by the AFM, and an AFM topographic image was generated (Fig. S3b, Supporting Information). Sites were picked at regular intervals on the scanned area (yellow dots in Fig. S3b, Supporting Information), and these sites were revisited for each electrolyte solution. Force measurements were thus conducted at 36 uniformly separated points in a 20 μm × 20 μm area as shown in Fig. S3 (Supporting Information). The force profiles reported here represent the average of the 36 point profiles collected in the 20 μm × 20μm area.

The raw data of force curves obtained in the voltage was converted to a force-distance curve. The method is described in Text S3 (Supporting Information).

2.4. DLVO model parameters

The DLVO model we employ uses the Derjaguin approximation that improves the Van der Waals attraction [31,32]. The implementation we use does not include steric or hydration forces. The model requires specification of the diameter of the SiO_2 colloid tip, the surface charge on the calcite and the colloid, the dielectric constant of water, and a Hamaker constant characterizing the interaction between SiO_2 and calcite. The diameter of the SiO_2 colloid is 5 μm. The surface charge on the silica colloid does not depend on the solution composition. Because there are only negative hydroxyl groups on SiO_2 surfaces, surface complexation or specific adsorption is very weak for SiO_2. In our calculation, the surface potential of SiO_2 colloid is kept constant at −60 mV (the value suggested by Wengeler et al. [38]) for all our solution compositions. The surface charge on the calcite depends on the solution composition and we treat it as a free parameter in the DLVO model. Bergström found the pure water Hamaker constant for calcite interacting against silica is 6.9×10^{-21} N m [39]. The Hamaker constant is slightly reduced in electrolyte solutions compared to pure water [40]. We find that the Hamaker constant for the SiO_2 AFM tip that works best in interpreting our experiments is 1.74×10^{-21} N m for the NaCl solutions and 1.50×10^{-21} N m in Na_2SO_4 solutions. A noticeably poor overall match between DLVO predictions and AFM measurements would be obtained by a Hamaker constant different from these values by greater or less than 0.5×10^{-21} N m.

3. Results and discussion

3.1. In NaCl solutions

Fig. 1 shows the ratio of collected to injected SiO_2 concentration as a function of the number of pore volumes of solution passed through the calcite sand-packed column. At $t = 0$, a 2.6 pore volume slug of SiO_2 nanoparticles dispersed in pure water or NaCl solutions was injected into the column. The SiO_2 particles were detected in the column effluent at 0.8 rather than 1 PV because there is some dispersion. After first detection, the effluent SiO_2 concentration depends on the concentration of NaCl in the solution, as shown in Fig. 1a.

SiO_2 particles that are dispersed in pure water increase in concentration very quickly in the effluent and reach the injected concentration at 1.3 PV. The 2.6 PV tracer slug is followed by DI water injection, and the SiO2 particle concentration starts to decreases at 3.3 PV and drops to zero at 4 PV. The distribution of early arrival and small tail around the plug flow reference is the same as the tracer arrival, and the recovery of the particle tracer is nearly 100%. The form of the pulse is nearly exactly the same as that in the Na_2SO_4 experiments (Fig. 1b). We interpret that the spread (non-sharp) arrival and termination of the particle tracer slug is caused by dispersion and that the pure water concentration pulse and the pulses in the Na_2SO_4 experiments represent a perfectly non-interacting particle tracer.

The concentration of SiO_2 particles dispersed in 0.5 mM NaCl solution increase less quickly than the particles dispersed in DI water, and the increase is diminished as the NaCl concentration increases. The particle concentrations all decrease along the same trajectory at the end of the tracer pulse, however. This suggests that the particles are simply retained in the column, and retained more in the more concentrated the NaCl solutions. The particle

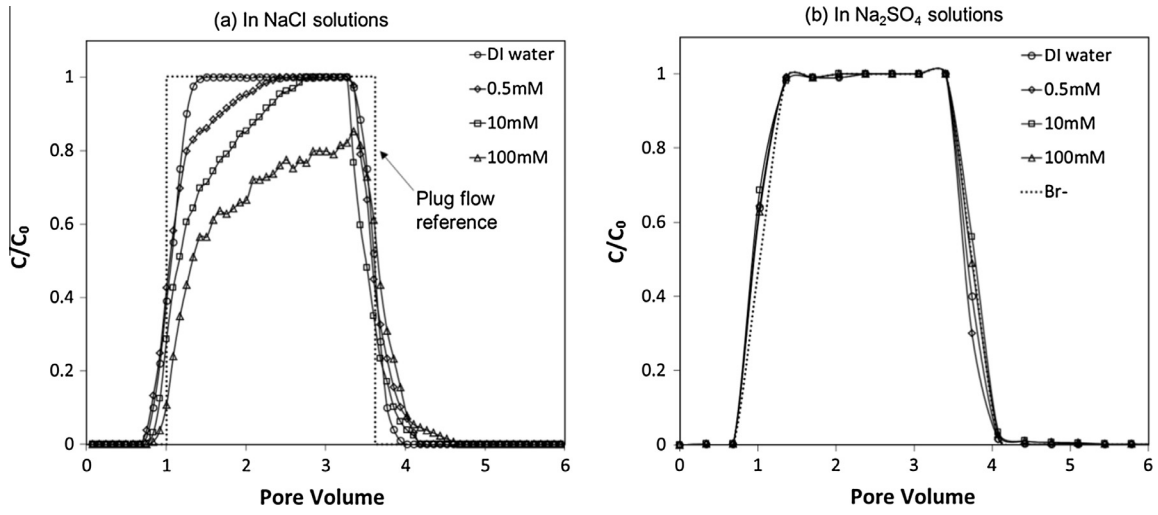

Fig. 1. The SiO_2 particle concentration in the column effluent as a fraction of the injected concentration in (a) NaCl solution and (b) Na_2SO_4 solution of varying NaCl or Na_2SO_4 molarity (0–100 mM) as a function of injection pore volume. The dashed curve in (a) is a plug flow reference curve. In all cases, a slug of 2.6 PV silica solutions was injected followed by particle-free solution of the same NaCl or Na_2SO_4 molarity.

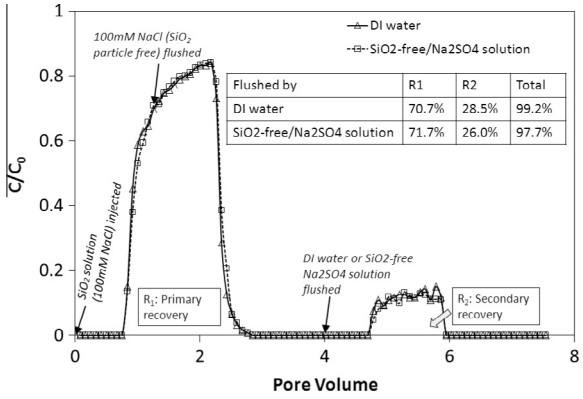

Fig. 2. The SiO_2 particle concentration in the column effluent as a fraction of the injected concentration in 100 mM NaCl solution as a function of injection pore volume. A slug of a 1.2 PV silica solution (100 mM NaCl) was injected followed first by 2.8 PV particle-free 100 mM NaCl solution and secondly by 3.6 PV DI water or particle-free 0.5 mM Na_2SO_4 solution. The particle recovery is shown in the insert table.

recovery was 95.6% for the 0.5 mM NaCl solution, 86.1% for the 10 mM NaCl solution, and 71.5% for the 100 mM NaCl solution.

3.2. In Na_2SO_4 solutions

Similar tracer experiments were run for silica particles in Na_2SO_4 solutions. Fig. 1b shows the ratio of collected to injected SiO_2 particle concentrations in the column effluent as a function of the number of pore volumes of Na_2SO_4 solution passed through the calcite sand-packed column for different Na_2SO_4 concentrations. The dotted line shows the effluent concentration of an inert KBr tracer. In the four experiments shown, the injected Na_2SO_4 concentration was 0 mM (in DI water), 0.5 mM, 10 mM, and 100 mM. The curves are all superimposed and overlie the DI water curve and the recovery is nearly 100% in all cases. There is no retention of the SiO_2 particles at any Na_2SO_4 concentration.

3.3. Flushing with DI or Na_2SO_4 water

Fig. 2 shows that if DI water or a 0.5 mM Na_2SO_4 solution is injected at 4 PV in a 100 mM NaCl test, the retained particles are immediately and completely released. The introduction of DI water or the Na_2SO_4 solution removes the adsorbed SiO_2 nanoparticles. Before the introduction of the particle-free DI water the particle recovery was 70.7% and 29.3% of the injected particles were retained in the column. After 2PV of DI water injection, an additional 28.5% of the particles injected have been recovered and the total particle recovery is 99.2%. It is similar for the case of flushing with Na_2SO_4 solutions of any molality. Before the flushing by the SiO_2-free Na_2SO_4 solution the particle recovery was 71.7% and 28.3% of the injected particles were retained in the column. After 2 PV of the SiO_2-free Na_2SO_4 solution injection, an additional 26.0% of the particles injected have been recovered and the total particle recovery is 97.7%.

The SEM images in Fig. 3 for the 100 mM NaCl experiment shown in Fig. 2 confirm that no SiO_2 particles remain adsorbed on the calcite surface after the DI water flushes the column, although many SiO_2 nanoparticles can be seen adsorbed on the calcite surface for an experiment where the column was not flushed with DI water at the close of the experiment.

3.4. AFM force profiles

Fig. 4a shows AFM interfacial force measurements between a silica colloidal probe and a calcite crystal submerged in NaCl solutions ranging from 0 mM to 100 mM. For $\leqslant$10 mM NaCl solutions, repulsion is measured between 0.6 nm and 10 nm from the calcite surface, and attraction when the tip is <0.6 nm from the surface. The magnitude of electrostatic repulsion decreases as the NaCl concentration increases. At the high NaCl concentrations (25–100 mM NaCl) only attraction is detected. The repulsion is strongest in dilute solution and is very small or absent when the NaCl concentration is larger than 10 mM. The force profiles are the average measurements of 36 locations shown as in Fig. S3b (Supporting Information). The standard deviation of the force profiles from the mean increases from 1% to 15% as the NaCl concentration increases. For a given concentration NaCl solution, the force curves vary for the different locations. Although the average (of all 36 locations) force curves in low ionic strength solutions (0–10 mM) show repulsion transitioning to attraction as the distance from the calcite surface decreases, at individual locations, however, some of the measured force curves show only attraction without any distal repulsion.

Fig. 4b shows force profiles between the SiO_2 colloid probe and the calcite surface when the calcite is submerged in Na_2SO_4 solution. Only repulsive forces are measured when the concentration of Na_2SO_4 is in the range of 0.5–100 mM. The magnitude of the repulsive force increases as the Na_2SO_4 concentration increases. In contrast to the NaCl case, there is little variation of force curve shape at the 36 different measured locations for a given Na_2SO_4 concentration,

3.5. Surface charge of calcite determined by DLVO model

The match between the DLVO predictions and the force measured between the SiO_2 AFM colloid tip and calcite immersed in NaCl solutions is shown in Fig. S4 (Supporting Information). The match for calcite submerged in Na_2SO_4 solutions is shown in

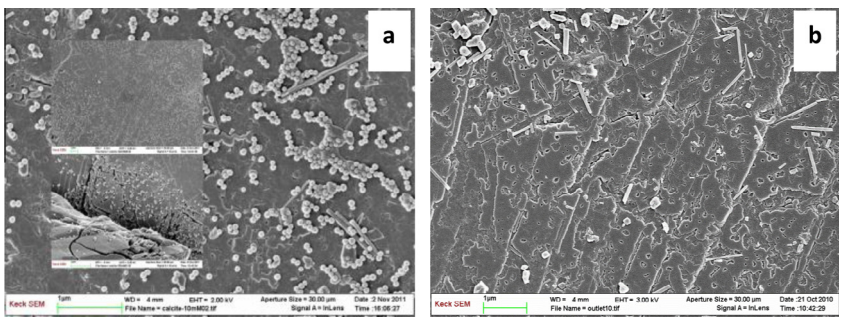

Fig. 3. SEM images show (a) silica nanoparticles remain adsorbed on calcite surface after the injection of a slug of 100 mM NaCl nanoparticle solution followed by particle free 100 mM NaCl. (b) No silica nanoparticles are observed on the calcite surface after a similar experiment where at the end of the experiment the column was flushed with DI. The DI water removed the silica particles which had been adsorbed on the calcite surface.

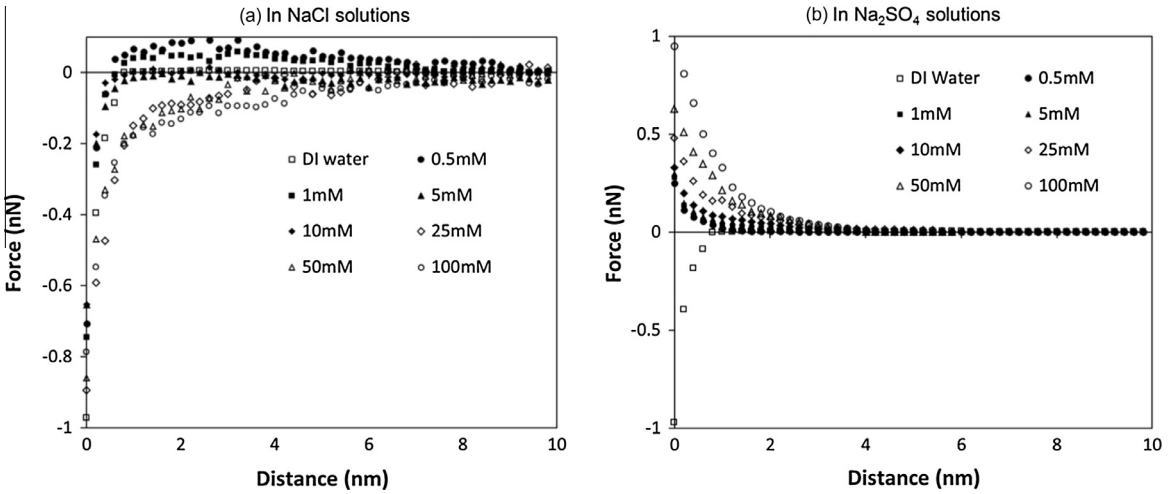

Fig. 4. Force curves between the SiO_2 AFM tip and a calcite surface that is immersed in DI water and in (a) NaCl solutions and (b) Na_2SO_4 solutions ranging from 0.5 mM to 100 mM NaCl. (a) At the low concentrations (0.5–10 mM NaCl) repulsion is detected before attraction takes over as the probe moves closer to the calcite surface. (b) The magnitude of the repulsion increases as the ionic strength of the Na_2SO_4 solution increase.

Fig. S5 (Supporting Information). The surface charge on the calcite needed to achieve these matches is shown in Fig. 5. Fig. 5a shows the calcite surface is negatively charged in the low ionic strength NaCl solutions (<10 mM), but becomes positively charged in higher ionic strength solutions. Fig. 5b shows surface charge of the calcite surface predicted by the DLVO model submerged in Na_2SO_4 solutions of various ionic strengths is negative, and becomes more negative as the ionic strength of the Na_2SO_4 solution increases.

Both the predicted force magnitude and the distance at which interaction forces become significant between the silica colloid and the flat calcite surface submerged in NaCl solutions predicted by the DLVO model are in good agreement with the AFM measurements (Fig. S4, Supporting Information). The DLVO model predicts the distance (<0.3 nm) at which the force becomes strongly attractive.

Fig. S5 (Supporting Information) shows the repulsive forces predicted by the DLVO model when the calcite is submerged in Na_2SO_4 solutions also agree well with the AFM measurements. However, the DLVO theory predicts strong attractive forces when the probe is closer than 0.3 nm from the calcite surface but the AFM probe fails to measure this expected VdW attraction. In DI water, the charge on the calcite predicted by our DLVO modeling of the force curve is −10 mV. The surface charge falls quickly as more NaCl is added to solution, and rises quickly (but remains negative) as more Na_2SO_4 is added.

The column experiments clearly illustrate the importance of solution chemistry in controlling the interaction of amorphous silica nanoparticles with calcite, and they are largely but not completely explained and interpreted by the AFM measurements. Silica nanoparticles are not retained in a granular calcite packed column when they are dispersed in a Na_2SO_4 solution or if they are dispersed in DI water (Fig. 1b). The AFM measurements show that when the calcite plate submerged in a Na_2SO_4 solution there is a strong electrostatic repulsion between the SiO_2 tip of the AFM probe. The repulsion increases as the concentration of the Na_2SO_4 increases (Fig. S5, Supporting Information). The very low retention

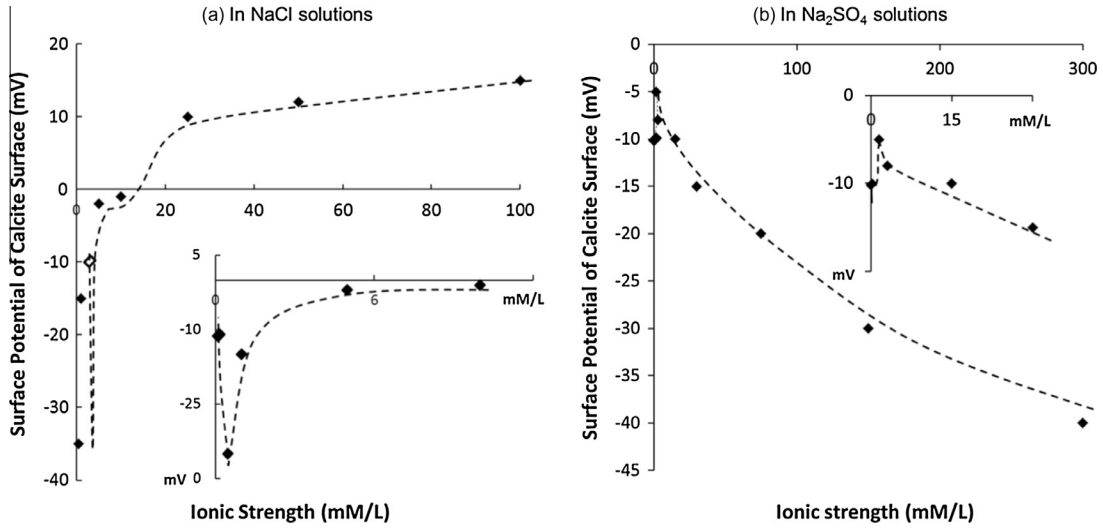

Fig. 5. Surface potential of calcite surface predicted by DLVO model as a function of ionic strength of (a) NaCl solution and (b) Na_2SO_4 solution (0–100 mM). The DLVO predictions are represented as diamonds connected by light dash lines. The change in the calcite surface potential suggests that the calcite surface immersed in NaCl solution is negatively charged in low ionic strength solution (<10 mM) but becomes positive when the ionic strength is greater than 10 mM. The change in the calcite surface potential suggests that the calcite surface immersed in Na_2SO_4 solution is negatively charged in the solution with the tested ionic strength (0–100 mM). The charge on the SiO_2 AFM tip is assumed constant.

of SiO_2 particles on calcite in a Na_2SO_4 and DI solution is thus explained by the absence of attraction.

When the silica nanoparticles are dispersed in NaCl solutions the situation is more complicated, as discussed earlier, but the explanation for retention remains electrostatic attraction. Fig. 1a shows that silica nanoparticles are not retained when dispersed in pure water, are retained slightly at low NaCl concentrations, and are retained more as the NaCl concentration increases. The particle retention is durable in the sense that flushing the column with many pore volumes of particle-free solution of the same salinity does not mobilize any of the retained particles.

3.6. Particle retention mechanism

The column and AFM measurements are broadly compatible and consistent with electrostatic attraction being the main factor controlling particle–calcite adhesion, but there are details that require explanation. SiO_2 particles dispersed in 0.5 mM NaCl solutions are significantly retained in the column tests even though the AFM measurements indicate repulsion. On the other hand, SiO_2 particles are not retained when they are dispersed in DI water, even though the AFM force profile shows no measureable electrostatic repulsion. It is curious also that the surface charge changes so dramatically with just a very little addition of NaCl or Na_2SO_4 to the solution. The fact that retained SiO_2 particles can be flushed when the chemistry of the fluid is changed suggests that the particle retention is not caused by VDW attraction, but electrostatic attraction. Surface charge on a mineral depends on the chemistry of the aqueous solution in which it is immersed, and if the particles are bound to the calcite by electrostatic forces it is logical that they could be released when the water chemistry is changed. The fact that the retention is partial and saturates with further injection (Fig. 1a), as well as the individual AFM measurements discussed above, suggests that part of the calcite surface has positive charge although most of the surface has negative charge. The column experiments suggest that the fraction of the calcite surface with positive charge retains the particles, and this fraction increases as the NaCl concentration increases.

A calcite crystal immersed in DI water undergoes some dissolution [41,42]. Calcium or carbonate ions could escape from the solid surface and diffuse into bulk solution, resulting in vacancies on the surface. Cygan et al. calculated the energy of formation of vacancies when one of the calcite ions is removed an infinite distance from the calcite crystal. This energy is called the defect energy, and for calcite in DI water it equals 20.53 eV for the formation of a Ca^{2+} vacancy, and 28.17 eV for the formation of a CO_3^{2-} vacancy, respectively [41]. This suggests that Ca^{2+} vacancies will be more prevalent for calcite in DI water, and the surface charge of calcite will be negative. The surface will attract a double layer consisting first of H^+ ions and then OH^- ions. Since these ions have very low concentration in DI water, it is reasonable that the surface charge and zeta potential will be very small, and this could explain the essentially zero repulsion observed by the AFM. Despite the small negative surface potential, it is apparently sufficient to keep the negatively charged silica particles from sticking to the calcite surface. When NaCl is added to the solution, Na^+ ions will be attracted to the Ca^{2+} vacancies, it is reasonable that the surface will become more strongly negatively charged, as observed in Fig. 4a. A scheme as shown in Fig. 6a illustrates the formation of Ca^{2+} vacancies and later the formation of a DLVO electrostatic double layer in dilute NaCl solutions.

Why, however, would the surface charge become less negative and eventually positive as the concentration of NaCl increases further? Fig. 6b shows a proposed explanation. We hypothesize that the increased abundance of Na^+ ions will complex with CO_3^{2-}, reduce the concentration of CO_3^{2-}, and encourage the formation of more CO_3^{2-} vacancies. The double layer adjacent to these vacancies will consist of Cl^- near the surface and then Na^+, giving a positive zeta potential that will attract and immobilize the negatively-charged SiO_2 particles. This explains why the retention increases as the NaCl concentration increases.

The Na_2SO_4 experiments and measurement have a completely different explanation. Dissolution of the calcite is unimportant compared to the consequences of SO_4^{2-} adsorption on the calcite surface. Sulfate is known to have a strong impact on the surface potential of calcium carbonate [43]. Sulfate adsorption changes the zeta potential of calcium carbonate from positive to negative at pH < 7. Using electroacoustic technology (AcoustoSizer), Zhang et al. measured

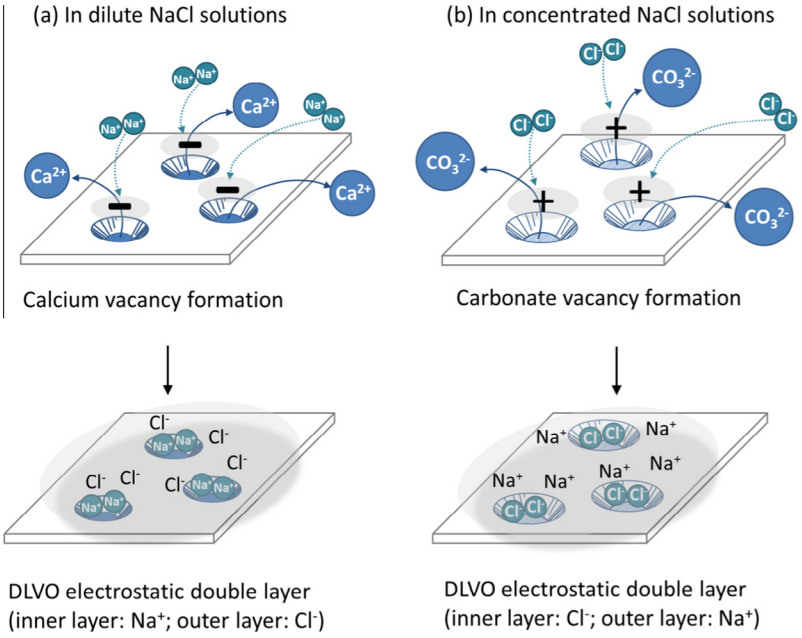

Fig. 6. Illustration of the formation of ion vacancy. (a) In dilute NaCl solutions, Ca^{2+} vacancies are formed resulting a first Na^+ and then Cl^- DLVO electrostatic double layer. (b) In concentrated NaCl solutions, CO_3^{2-} vacancies are formed resulting a first Cl^- and then Na^+ DLVO electrostatic double layer.

the zeta potential of chalk powder in solutions containing both NaCl and Na_2SO_4, and reported negative zeta potentials in a range of −10 mV to −25 mV [19]. The pH in their solution was 8.4 which is similar to that of our solution. Hiorth et al. theoretically predicted the zeta potential for the same water chemistries used in Zhang's experiments, and obtained negative zeta potentials that agree well with Zhang's measurements [18]. These experiments and models suggest that sulfate ions are adsorbed on the calcium carbonate surfaces when Na_2SO_4 is present in the aqueous solution, making the calcite surface charge negative. This negative calcite surface will attract Na + ions and the outer part of the double layer will be SO_4^{2-} ions, giving a negative zeta potential that will repel negatively charged silica particles. We have no good explanation for why the AFM silica probe sees no VdW attraction, other than that the electrostatic repulsion of the adsorbed SO_4^{2-} for the SiO_2 tip may overwhelm the VdW forces.

4. Conclusions

We report column experiments that indicate surface charge is a primary cause of particle retention in porous media, confirming indications from an earlier screening paper [34]. We measure the retention of commercial SiO_2 nanoparticles when they are dispersed in NaCl or Na_2SO_4 solutions and passed through laboratory columns packed with calcium carbonate sand. The SiO_2 particles show no retention when dispersed in DI water or Na_2SO_4 solutions. By contrast the particles are significantly retained when dispersed in NaCl solutions, and the retention, significant at even low NaCl concentration, increases with the ionic strength of the solution. The retained particles are stably retained in the sense that continued flushing with the same chemistry solution does not remove them. However, if the solution chemistry is changed to one for which the particles are not retained, the particles are immediately released. As far as we know, no one has previously drawn attention to this phenomenon.

AFM measurements and DLVO theory support the hypothesis that the silica particles are retained on the portions of the calcite surface where they are electrostatically attracted. Retention increases with NaCl concentration because the additional Na+ complexes with CO_3^{2-} and decreases the molality of CO_3^{2-}, causing more CO_3^{2-} vacancies to form. Sulfate adsorption, a very different process than calcite dissolution, controls the surface charge of calcite in Na_2SO_4 solutions,

There are three broad implications of this work: First, since subsurface minerals are likely to have areas of positive and areas of negative charge, the most inert particle tracers should have no charge. Second, experiments measuring particle retention are useful to understanding surface charge. Lastly, AFM measurements are useful to understanding the causes of particle retention on mineral surfaces.

Future work might use particle retention to study how the surface charge changes with solution chemistry and how charge distribution changes on different cleavage faces. Our 5 mm diameter silica probe tip detected different charge at different locations on the cleaved calcite surface. It would be interesting to see if a smaller tip would detect larger charge variations and perhaps even map the pattern of positive and negative surface charge, and it would be interesting to examine differences in charge intensity and pattern between surfaces with different cleavage orientation.

Another avenue of investigation would be to measure retention in columns packed with different size and shape calcite grains. Calcite grain shape could affect retention. Whether smaller nanoparticles have less retention (another suggestion in Li et al. [34]), and the role of hydrophilic decoration in reducing retention are outstanding issues, some of which we are currently addressing.

Acknowledgments

This publication is based on work supported by Aramco Services Company (Project ID: ASC #660022190) and by Award No. KUS-C1-018-02 from the King Abdullah University of Science and Technology. Support was also provided by a general fund contribution to L. Cathles from The International Research Institute of Stavanger. The authors appreciate Prof. Tracy Bank at SUNY at Buffalo for her priceless discussion on DLVO modeling.

Appendix A. Supplementary material

More information is available for the materials and analysis. This material is available free of charge via the Internet at http://pubs.acs.org. Supplementary data associated with this article can be found, in the online version, at http://dx.doi.org/10.1016/j.jcis.2014.08.072.

References

[1] A.R. Petosa, D.P. Jaisi, I.R. Quevedo, M. Elimelech, N. Tufenkji, Environ. Sci. Technol. 44 (17) (2010) 6532–6549.
[2] M. Colombo, S. Carregal-Romero, M.F. Casula, L. Gutierrez, M.P. Morales, I.B. Bohm, J.T. Heverhagen, D. Prosperi, W.J. Parak, Chem. Soc. Rev. 41 (11) (2012) 4306–4334.
[3] A. Albanese, P.S. Tang, W.C.W. Chan, Annu. Rev. Biomed. Eng. 14 (1) (2012) 1–16.
[4] H.M. Chen, R.-S. Liu, J. Phys. Chem. C 115 (9) (2011) 3513–3527.
[5] Y. Yin, D. Talapin, Chem. Soc. Rev. 42 (7) (2013) 2484–2487.
[6] B. Bharti, J. Meissner, U. Gasser, G.H. Findenegg, Soft Matter 8 (24) (2012) 6573–6581.
[7] J.D. Trono, K. Mizuno, N. Yusa, T. Matsukawa, K. Yokoyama, M. Uesaka, J. Radiat. Res. 52 (1) (2011) 103–109.
[8] A. Panáček, R. Prucek, J. Hrbáč, T.j. Nevečná, J. Šteffková, R. Zbořil, L. Kvítek, Chem. Mater. 26 (3) (2014) 1332–1339.
[9] S. Thongrattanasiri, F.H.L. Koppens, F.J. García de Abajo, Phys. Rev. Lett. 108 (4) (2012) 047401.
[10] M. Pauly, B.P. Pichon, P. Panissod, S. Fleutot, P. Rodriguez, M. Drillon, S. Begin-Colin, J. Mater. Chem. 22 (13) (2012) 6343–6350.
[11] J.E. Gagner, M.D. Lopez, J.S. Dordick, R.W. Siegel, Biomaterials 32 (29) (2011) 7241–7252.
[12] S. Pal, Y.K. Tak, J.M. Song, Appl. Environ. Microbiol. 73 (6) (2007) 1712–1720.
[13] J.M. Pettibone, D.M. Cwiertny, M. Scherer, V.H. Grassian, Langmuir 24 (13) (2008) 6659–6667.
[14] B. Bharti, J. Meissner, S.H.L. Klapp, G.H. Findenegg, Soft Matter 10 (5) (2014) 718–728.
[15] H.P. van Leeuwen, J. Buffle, J.F.L. Duval, R.M. Town, Langmuir 29 (33) (2013) 10297–10302.
[16] G. Chen, X. Liu, C. Su, Langmuir 27 (9) (2011) 5393–5402.
[17] A.J. Pelley, N. Tufenkji, J. Colloid Interface Sci. 321 (1) (2008) 74–83.
[18] A. Hiorth, L. Cathles, M. Madland, Transp. Porous Media 85 (1) (2010) 1–21.
[19] P. Zhang, T. Austad, Colloids Surf., A 279 (1–3) (2006) 179–187.
[20] P. Christian, F. Von der Kammer, M. Baalousha, T. Hofmann, Ecotoxicology 17 (5) (2008) 326–343.
[21] E. Rodriguez, M.R. Roberts, H. Yu, C. Huh, S.L. Bryant, Enhanced migration of surface-treated nanoparticles in sedimentary rocks, in: SPE Annual Technical Conference and Exhibition, Society of Petroleum Engineers: New Orleans, Louisiana, 2009, pp. 21. doi: http://dx.doi.org/10.2118/124418-MS.
[22] R.A. Crane, T.B. Scott, J. Hazard. Mater. 211–212 (2012) 112–125.
[23] M.V. Liga, E.L. Bryant, V.L. Colvin, Q. Li, Water Res. 45 (2) (2011) 535–544.
[24] A.K. Dutta, S.K. Maji, B. Adhikary, Mater. Res. Bull. 49 (2014) 28–34.
[25] R.W.N. Nugroho, T. Pettersson, K. Odelius, A. Höglund, A.-C. Albertsson, Langmuir 29 (28) (2013) 8873–8881.
[26] E. Guzmán, L. Liggieri, E. Santini, M. Ferrari, F. Ravera, J. Phys. Chem. C 115 (44) (2011) 21715–21722.
[27] L. He, M. Wang, J. Ge, Y. Yin, Acc. Chem. Res. 45 (9) (2012) 1431–1440.
[28] A. Ravindran, A. Singh, A.M. Raichur, N. Chandrasekaran, A. Mukherjee, Colloids Surf., B 76 (1) (2010) 32–37.
[29] W. Zhang, A.G. Stack, Y. Chen, Colloids Surf., B 82 (2) (2011) 316–324.
[30] R. Frost, S. Svedhem, Characterization of nanoparticle–lipid membrane interactions using QCM-D, in: V. Weissig, T. Elbayoumi, M. Olsen (Eds.), Cellular and Subcellular Nanotechnology, 991, Humana Press, 2013, pp. 127–137.
[31] T.L. Cail, M.F. Hochella Jr., Geochim. Cosmochim. Acta 69 (12) (2005) 2959–2969.
[32] T.L. Cail, M.F. Hochella, Environ. Sci. Technol. 39 (4) (2005) 1011–1017.
[33] S.K. Subramanian, Y. Li, L.M. Cathles, Water Resour. Res. 49 (1) (2013) 29–42.
[34] Y.V. Li, L.M. Cathles, L.A. Archer, J. Nanopart. Res. 16 (8) (2014) 1–14.
[35] A.O. Harstad, S.L.S. Stipp, Geochim. Cosmochim. Acta 71 (1) (2007) 56–70.

[36] H.N. de Leeuw, S.C. Parker, Atomistic simulation of the effect of molecular adsorption of water on the surface structure and energies of calcite surfaces, J. Chem. Soc., Farad. Trans. 93 (3) (1997) 467–475.
[37] I.G. Godinez, C.J.G. Darnault, Water Res. 45 (2011) 13.
[38] R. Wengeler, Hydrodynamic Stress Induced Dispersion of Nanoscale Agglomerates By a High Pressure Process, Cuvillier Verlag, Göttingen, 2006. p 173.
[39] L. Bergström, Adv. Colloid Interface Sci. 70 (1997) 125–169.
[40] Y.U. Moon, C.O. Anderson, H.W. Blanch, J.M. Prausnitz, Fluid Phase Equilib. 168 (2) (2000) 229–239.
[41] R.T. Cygan, K. Wright, D.K. Fisler, J.D. Gale, B. Slater, Mol. Simul. 28 (6–7) (2002) 475–495.
[42] C. Fischer, R.S. Arvidson, A. Lüttge, Geochim. Cosmochim. Acta 98 (2012) 177–185.
[43] J.J. McDermott, A. Kar, M. Daher, S. Klara, G. Wang, A. Sen, D. Velegol, Langmuir 28 (44) (2012) 15491–15497.